BOR DERGİSİ
JOURNAL OF BORON
https://dergipark.org.tr/boron

Box–Behnken experimental design for zinc borate $Zn_2B_6O_{11}\cdot 7H_2O$

Sevgi Polat[1], Perviz Sayan[2]*

[1]Marmara University, Department of Chemical Engineering, 34722, Istanbul, Turkey, ORCID ID orcid.org/0000-0002-0934-2125
[2]Marmara University, Department of Chemical Engineering, 34722, Istanbul, Turkey, ORCID ID orcid.org/ 0000-0003-4407-6464

ARTICLE INFO

Article history:
Received 04 March 2020
Received in revised form 26 September 2020
Accepted 27 September 2020
Available online 30 September 2020

Research Article

DOI: 10.30728/boron.698858

Keywords:
Zinc borate,
Box–Behnken design,
Crystallization,
Morphology.

ABSTRACT

The present study investigated the effect of the operating conditions on the crystallization of zinc borate. For zinc borate crystallization, sodium tetraborate decahydrate and zinc sulfate heptahydrate were used as reactants. In the first part of the study, the crystals were characterized by X-ray diffraction spectroscopy (XRD), Fourier-transform infrared spectroscopy (FTIR), light microscopy, and particle size and thermogravimetric analysis. The results show that the obtained crystals were in the form of $Zn_2B_6O_{11}\cdot 7H_2O$, and the operating conditions had a significant effect on the size, morphology, and filtration characteristics of the zinc borate crystals. In the second part of the study, Box–Behnken design (BBD) with response surface methodology (RSM) was employed to determine the optimal operating conditions for zinc borate crystallization. The effects of stirring rate, temperature, and reactant feed rate on the average particle size were investigated. The results show that the data sufficiently fit the second-order polynomial model. The crystallization conditions, including stirring rate, temperature, and reactant feed rate, were studied at 400–500 rpm, 45–85 ºC, and 300–900 mL/h, respectively. The minimum particle size (3.3 µm) was obtained at a stirring rate of 450 rpm, a temperature of 85 ºC, and a reactant feed rate of 300 mL/h.

1. Introduction

Zinc can form several hydrated borates including $2ZnO\cdot 3B_2O_3\cdot 3.5H_2O$, $4ZnO\cdot B_2O_3\cdot H_2O$, $2ZnO\cdot 3B_2O_3\cdot 7H_2O$, $2ZnO\cdot 3B_2O_3\cdot 3H_2O$, $3ZnO\cdot 5B_2O_3\cdot 5H_2O$, and $ZnO\cdot 5B_2O_3\cdot 4.5H_2O$ [1]. Zinc borates have many important uses as ingredients in plastic, rubber, cement, glass, ceramic, electrical insulation, and even medicines. Moreover, zinc borates are employed as preservatives in wood composites, anticorrosive pigments in paint, and polymer additives for the promotion of char formation to suppress smoke and retard combustion [2-4]. Zinc borates are also commonly used as host lattices for photo- and thermoluminescent material phosphors as a result of their high thermal and chemical stability, convenient synthesis, and low cost. Furthermore, zinc borates can have applications in tribology and medicine [5]. Due to their use in different industries, a plethora of studies have been performed, showing that zinc borate crystallization affected by various physicochemical parameters [6-8] such as pH, temperature, supersaturation, operating conditions, and the presence of surface-modifying reagents [9-12].

In the present study, $Zn_2B_6O_{11}\cdot 7H_2O$ crystallization was investigated in detail. The crystal properties including morphology, phase structure, filtration characteristics, and average particle size were compared under different operating conditions. An experimental design technique was also applied to gain insight into the effects of the process variables of stirring rate, temperature, and feed rate on zinc borate crystal formation. Detailed identification of the combined effects of process variables on the crystallization of zinc borate crystals will provide useful information for various industries. The experimental data were analyzed by fitting to a quadratic model, the significance of which was determined by analysis of variance (ANOVA). The results obtained in the present study will contribute to the determination of the optimal conditions for processes in which zinc borate crystallization occurs under different working conditions. Moreover, the results of the characterization and optimization can be used as a guide for research regarding the control of zinc borate crystal size.

2. Materials and methods

The analytical-grade pure powdered sodium tetraborate decahydrate ($Na_2B_4O_7.10H_2O$) and zinc sulfate heptahydrate ($ZnSO_4.7H_2O$) were purchased from Merck. Distilled water was used in all experiments. All experiments were carried out at least in triplicate.

The zinc borate was synthesized by the reaction of

*Corresponding author: perviz.sayan@marmara.edu.tr

$Na_2B_4O_7.10H_2O$ with $ZnSO_4.7H_2O$ in a double-jacketed glass crystallizer containing an active volume of 500 mL. Temperature control within the crystallizer was provided by a thermostat, and stirring was performed by three-blade propellers at a constant stirring rate of 400 rpm controlled by a mechanical motor. The experimental setup is illustrated in Figure 1.

At the beginning of the experiments, $Na_2B_4O_7.10H_2O$ solution was prepared and to start the crystallization, the solution was placed into the crystallizer. After thermal equilibrium was reached, the $ZnSO_4.7H_2O$ solution was fed into the crystallizer via a peristaltic pump to produce zinc borate crystals. After the reactant had been added to the crystallizer, the suspension was left to stir for half an hour. At the end of this time, the crystallizer contents were filtered and washed thoroughly with distilled water. The washed zinc borate crystals were then dried at room temperature and subjected to various characterization processes. To investigate the effect of the temperature and feed rate of reactants on zinc borate crystallization, the experiments were performed at three different temperatures of 45, 65, and 85 °C, feed rates of 300, 600 and 900 mL/h, and stirring rates of 400, 450, and 500 rpm.

The structures of the prepared samples were identified by powder X-ray diffraction (XRD) analysis (Bruker D2 Phaser benchtop) using Cu Kα radiation (λ = 1.5418 Å). The scans were performed for 2θ values of 10–40°. The IR spectra were obtained using a Bruker Tensor 27 Fourier transform infrared (FTIR) spectrometer in the wavenumber range from 4000 to 400 cm^{-1}. The morphology of the zinc borate was observed using a light microscope. The crystal size was analyzed using a Malvern 2000 instrument. The thermal decomposition of the zinc borate was determined using a Netsch STA 409 thermogravimetric analyzer in nitrogen atmosphere between 25 °C and 800 °C with the heating rate of 10 °C/min. The filtration rate of the zinc borate crystals was measured using a Millipore standard laboratory vacuum filtration system at 110 mbar.

3. Results and discussion

3.1. XRD and FTIR analysis

The XRD patterns of the zinc borate crystals obtained at 450 rpm, 65°C, and 600 mL/h, in addition to the corresponding data from the JCPDS card, are presented in Table 1.

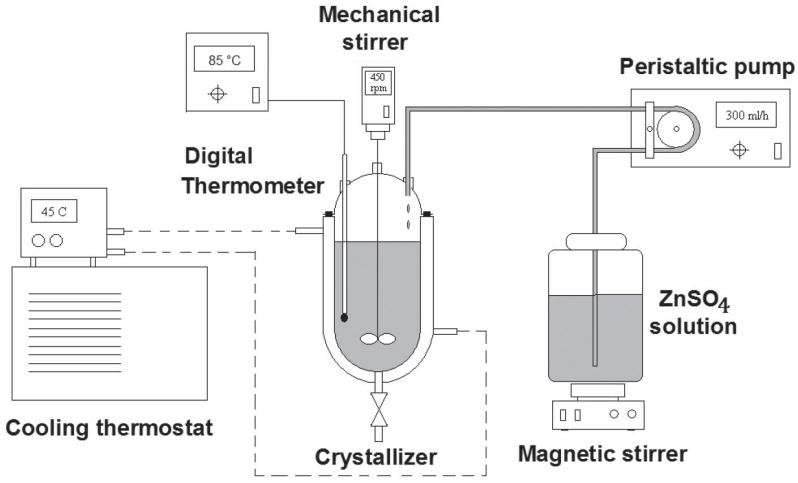

Figure 1. Experimental setup.

Table 1. XRD data of zinc borate crystals and the corresponding JCPDS card values.

Measured values			JCPDS cards values		
2θ (°)	d (Å)	I%	2θ	d (Å)	I%
13.281	6.6612	100	13.243	6.6800	100
17.759	4.9902	60	17.547	5.0500	60
19.840	4.4712	60	19.756	4.4900	60
21.162	4.1949	20	21.136	4.2000	20
23.420	3.7953	40	23.205	3.8300	40
25.701	3.4633	60	25.726	3.4600	60
26.600	3.3483	80	26.586	3.3500	80
29.620	3.0135	80	29.554	3.0200	80
31.220	2.8626	40	31.026	2.8800	40
33.439	2.6775	20	33.407	2.6800	20
35.838	2.5036	60	35.597	2.5200	60
36.881	2.4351	60	36.962	2.4300	60
38.420	2.3410	10	38.268	2.3500	10

The experimentally observed XRD data closely matched those of JCPDS: 32–1463, indicating that the obtained crystals were in the form of $Zn_2B_6O_{11}\cdot 7H_2O$.

FTIR analysis was performed to determine which functional groups were present in the samples. Figure 2 shows the FTIR spectra for zinc borate samples obtained at a temperature of 45, 65, and 85 °C at 600 mL/h. The peaks between 3000 and 3500 cm^{-1} were attributed to the O–H stretching vibration. The peak at 2505 cm^{-1} belonged to the O–H stretching due to the hydrogen bond. The peaks located at 1184 and 1268 cm^{-1} were ascribed to the in-plane bending of B–O–H. The medium band at 1389 cm^{-1} was due to $B_{(3)}$–O asymmetric stretching vibrations. The two bands at approximately 1021 and 883 cm^{-1} denoted the presence of

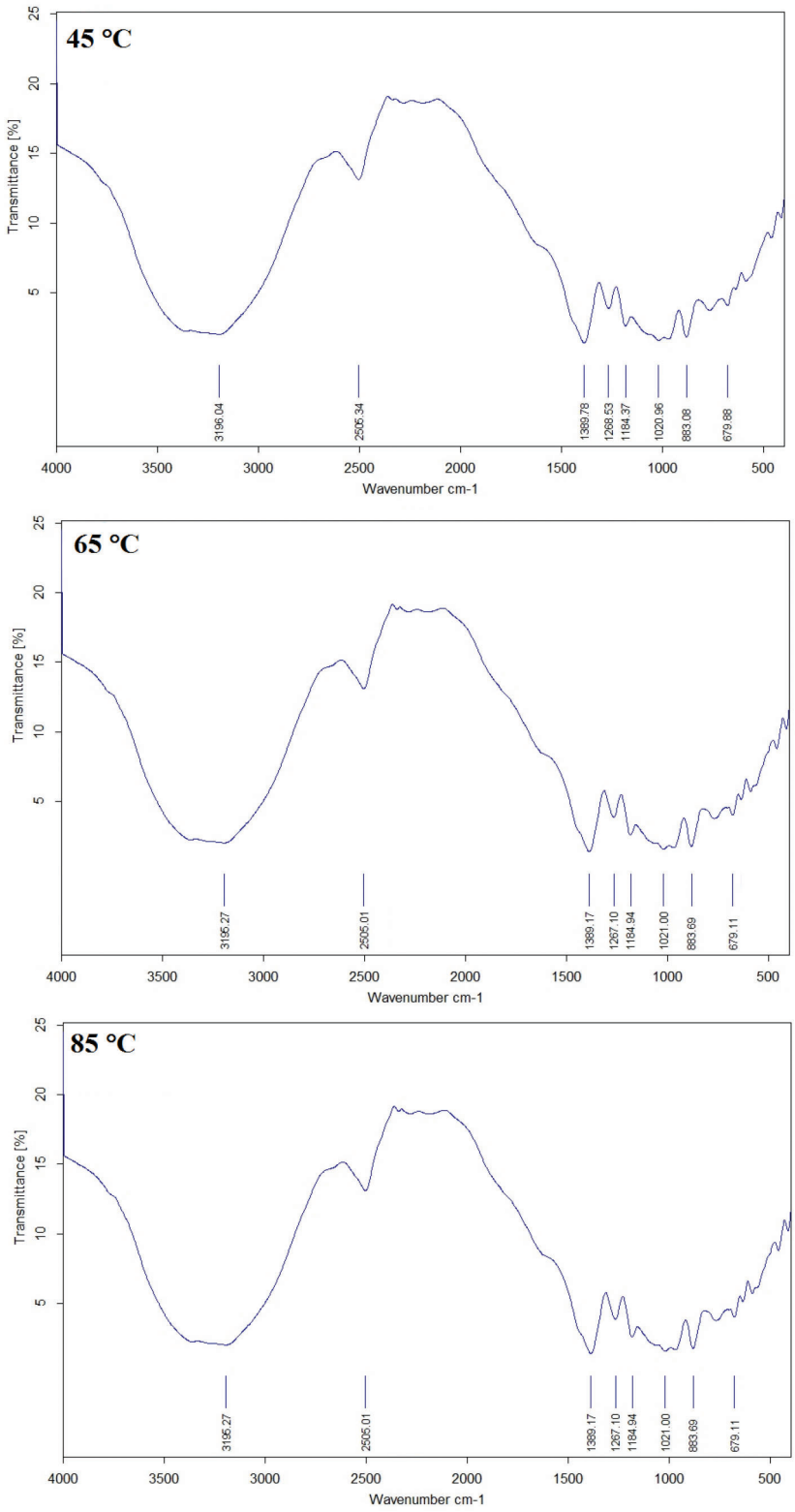

Figure 2. FTIR spectra for zinc borate samples obtained at different temperatures.

asymmetric and symmetric stretching of $B_{(4)}$–O, respectively. The peak at 679 cm^{-1} was associated with the out-of-plane bending mode of $B_{(3)}$–O [13,14]. Consistent with the XRD results, FTIR analysis shows that the crystals obtained at different temperatures were in the $Zn_2B_6O_{11}\cdot 7H_2O$ form.

3.2. Thermal analysis

The thermogravimetric (TG) and differential thermal analysis (DTA) curves for the obtained zinc borate at 450 rpm and 600 mL/h are presented in Figure 3 for experiments conducted at 45, 65 and 85 °C. In the DTA

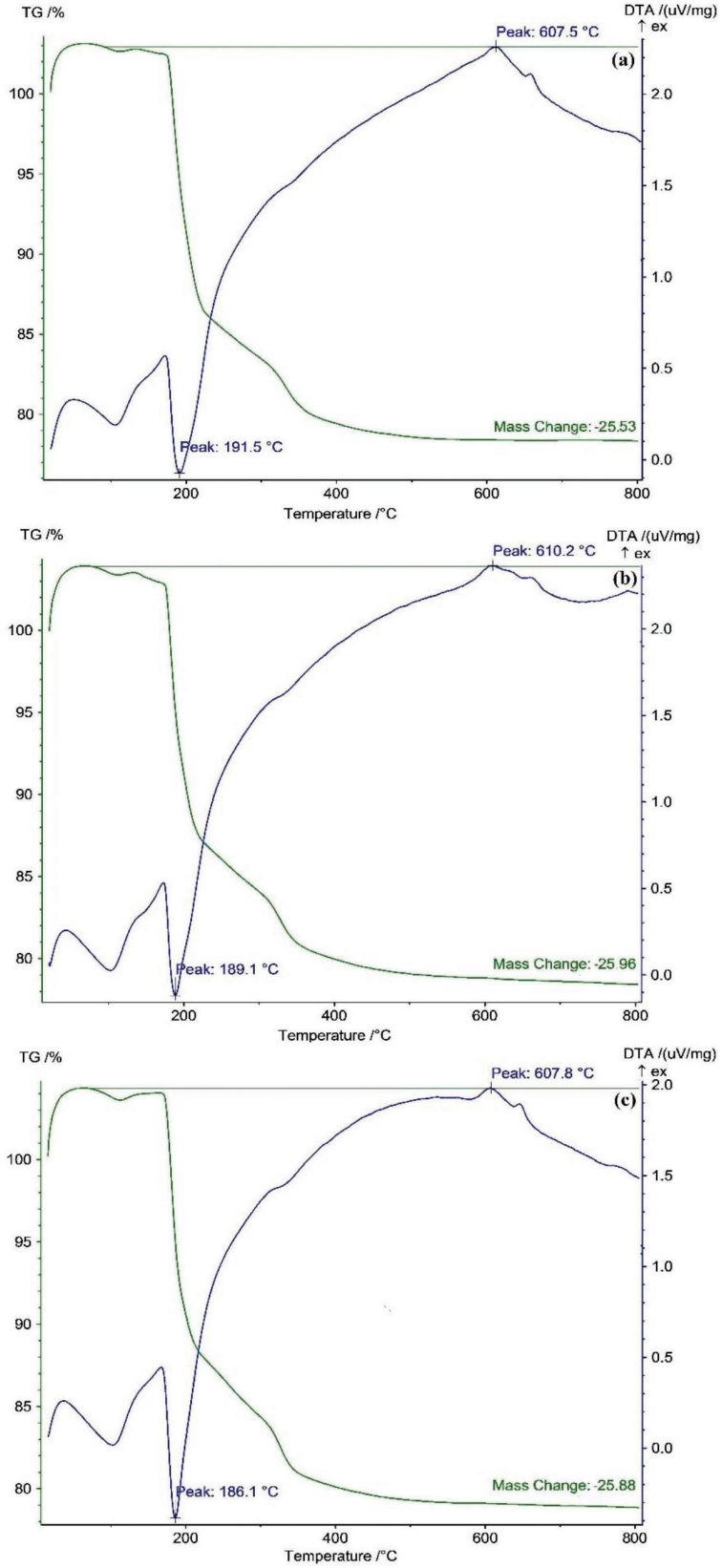

Figure 3. TG/DTA curves of the zinc borate obtained at 45 °C (a), 65 °C (b), and 85 °C (c).

curves, an endothermic peak was observed at approximately 190 °C, which was related to the elimination of crystalline water. An exothermic peak at approximately 610 °C was also detected. The formed amorphous phase of zinc borate recrystallized, as shown by the exothermic peak at approximately 610 °C [13]. During the thermal decomposition of zinc borate (between 30 and 800 °C), a total weight loss of 25.53, 25.96, and 25.88% was recorded at 45, 65, and 85 °C, respectively, which corresponds to the loss of seven water molecules, agreeing with the theoretical value.

3.3. Morphological analysis

The effects of the stirring rate, reactant feed rate, and temperature on zinc borate crystallization were investigated. Firstly, to determine the influence of the stirring rate, the experiments were carried out at three stirring rates of 400, 450, and 500 rpm and a constant temperature of 65 °C and a constant reactant feed rate of 600 mL/min. The results show that the stirring rate did not affect crystal morphology or particle size.

Figure 4 displays the microscopy images and corresponding particle size distributions of the zinc borate samples obtained at a temperature of 45, 65, and 85 °C at 300 mL/h, i.e., a low reactant feed rate.

As indicated in Figure 4, an increase in temperature led to a decrease in the average particle size of the crystals. At higher temperatures, deformation of the crystal surface occurred. A decrease in particle size with increasing temperature was similarly observed at

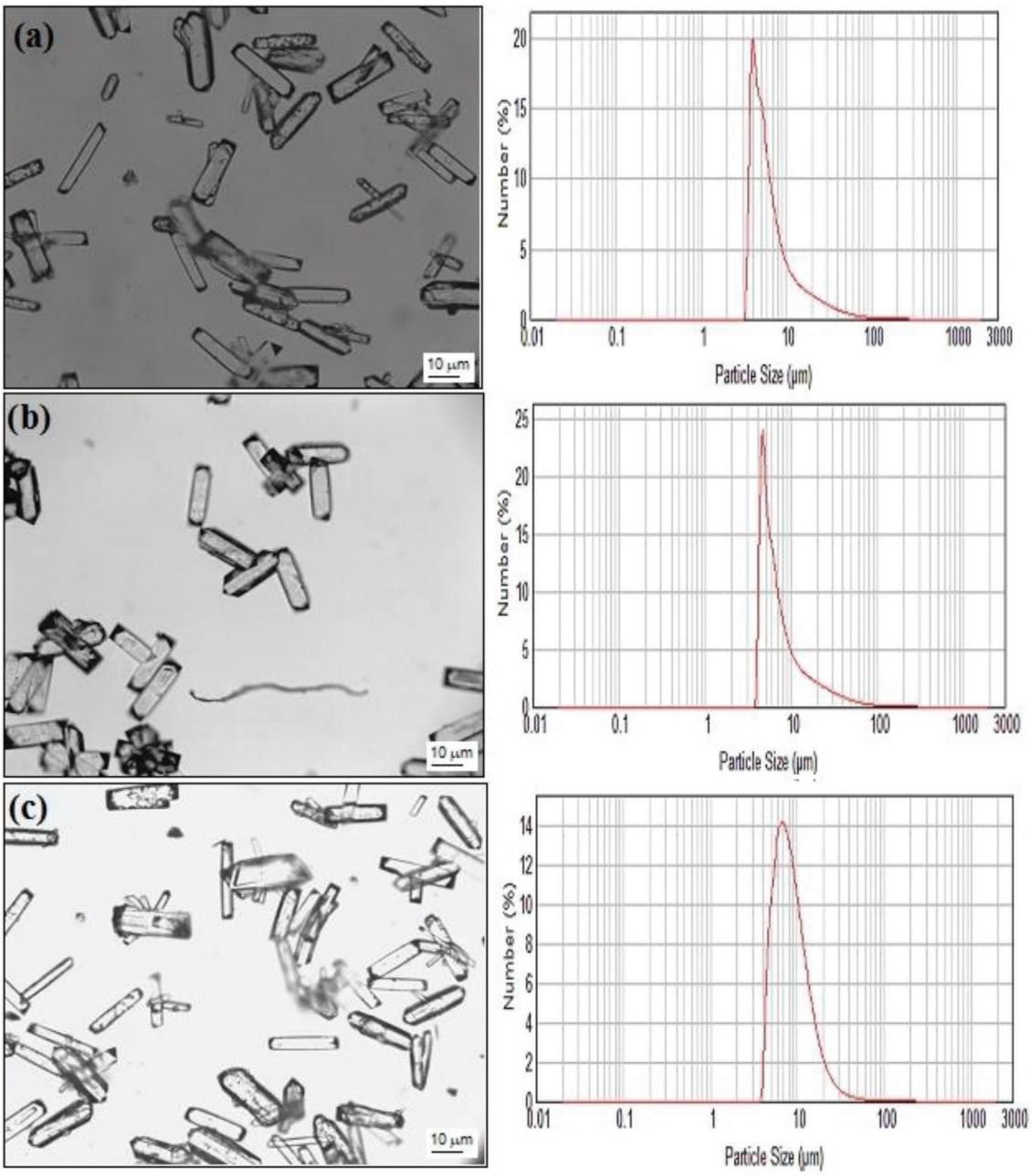

Figure 4. Microscopy images and corresponding particle size distributions of zinc borate obtained at a temperature of 45 °C (a), 65 °C (b), and 85 °C (c) at 300 mL/h.

the two other feed rates of 600 and 900 mL/h, the results of which are given in Figures 5 and 6. As can be clearly seen from the microscopy images, increasing the temperature caused crystal deformation and twinning behavior. Furthermore, the agglomeration tendency of the crystals increased at higher temperatures.

The crystal morphology of zinc borate crystals was also affected by the feed rate. In contrast to the effect of temperature, an increase in the feed rate contributed to the formation of zinc borate crystals of a larger particle size, mainly within the range of 10–100 μm. At a constant temperature of 65 °C and a constant stirring rate of 450 rpm, the particle size of the crystals was 4.7, 5.4, and 6.2 μm at 300, 600, and 900 mL/h, respectively. The zinc borate crystals were shortened in length and enlarged in width as the feed rate was increased. The aspect ratio of the crystals obtained at 65 °C and 300, 600, and 900 mL/h was determined to be 0.301, 0.312, and 0.345, respectively, by dividing the width of the crystal by its length. A further increase in temperature to 85 °C gave an average particle size of 3.3, 3.8, and 5.2 μm at 300, 600, and 900 mL/h, respectively

3.4. Filtration analysis

The effects of the operating conditions on the filtration characteristics of zinc borate were investigated in the present study. The filtration rate and specific cake resistance results are presented in Table 2.

The filtration results indicated that the significant differences between the cake resistance and filtration rates in the suspensions were influenced by the operating conditions studied. Among the investigated conditions,

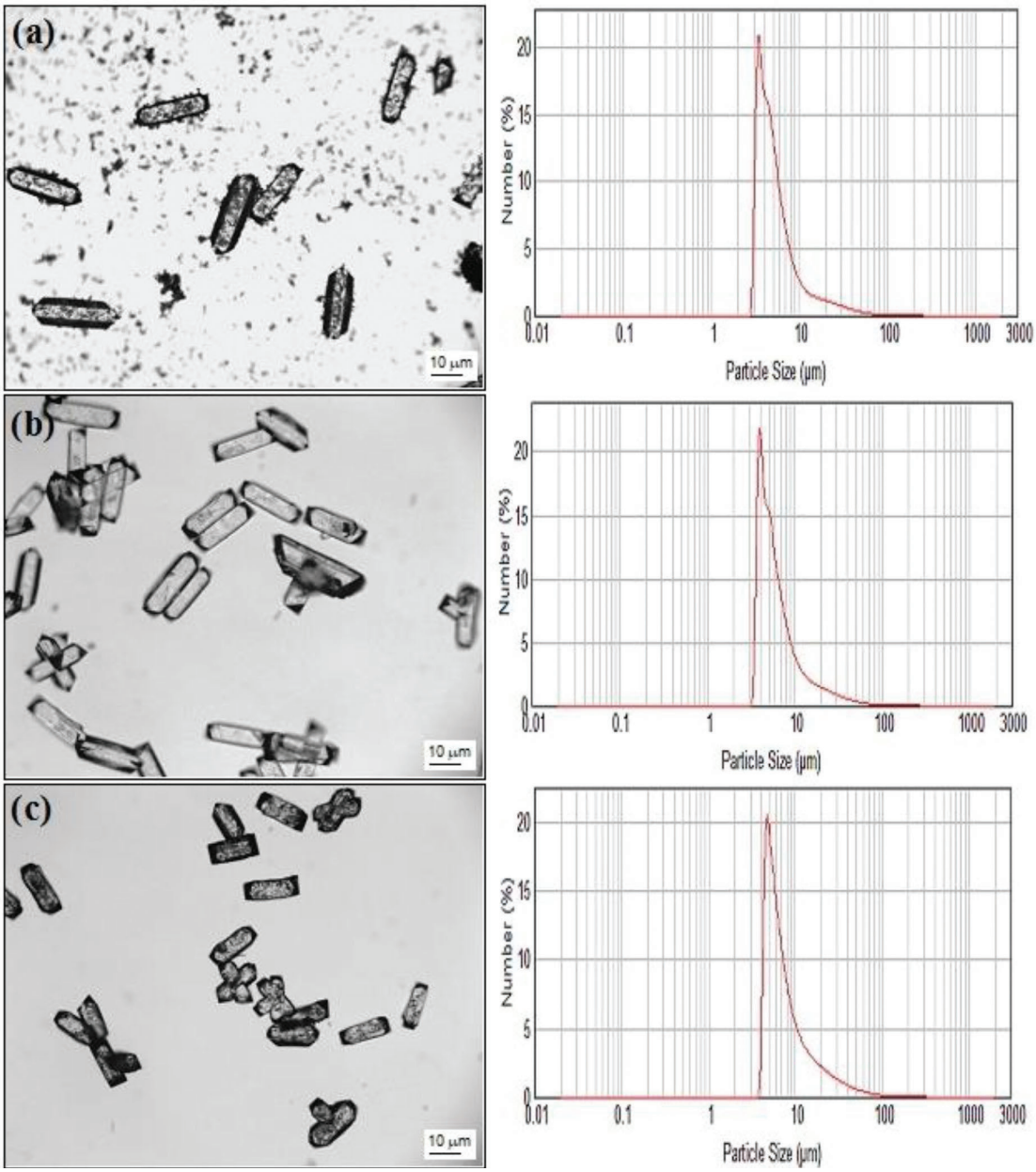

Figure 5. Microscopy images and corresponding particle size distributions of zinc borate obtained at a temperature of 45 °C (a), 65 °C (b), and 85 °C (c) at 600 mL/h.

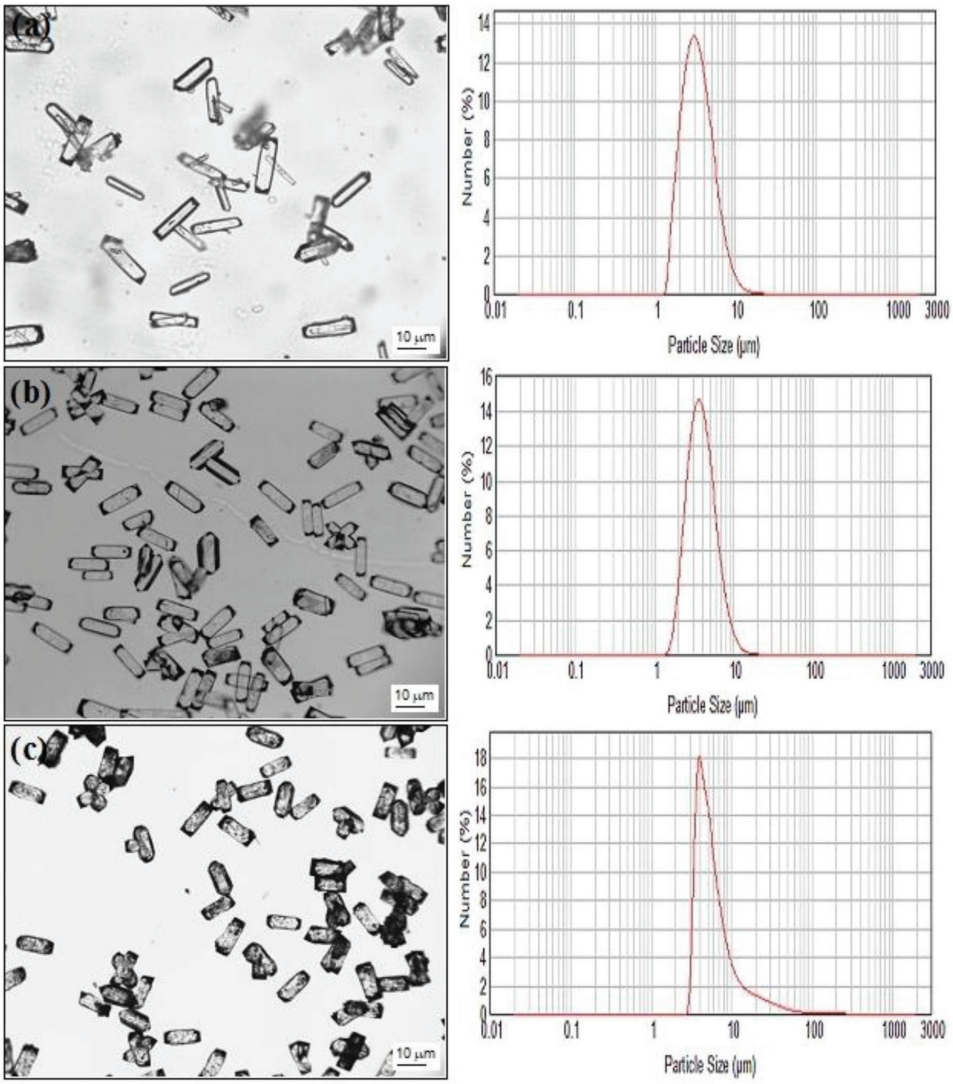

Figure 6. Microscopy images and corresponding particle size distributions of zinc borate obtained at a temperature of 45 °C (a), 65 °C (b), and 85 °C (c) at 900 mL/h.

Table 2. Filtration results of zinc borate.

Temperature (°C)	Feed rate (mL/h)	Specific cake resistance (m/kg)	Filtration rate (m^3/s)
45		1.89×10^{10}	4.41×10^{-8}
65	300	2.73×10^{10}	3.87×10^{-8}
85		2.94×10^{10}	2.84×10^{-8}
45		1.56×10^{10}	4.80×10^{-8}
65	600	2.07×10^{10}	4.03×10^{-8}
85		2.80×10^{10}	3.30×10^{-8}
45		1.33×10^{10}	5.52×10^{-8}
65	900	1.61×10^{10}	5.12×10^{-8}
85		1.97×10^{10}	3.85×10^{-8}

highest feed rate and lowest temperature were most efficient for filtration, obtaining the lowest cake resistances and highest filtration rate. As shown in Table 2, the highest filtration rate (5.52×10^{-8} m^3/s) and lowest specific cake resistance (1.33×10^{10} m/kg) were obtained at 45 °C and 900 mL/h feed rate. The changes in filtration characteristics can be attributed to the size and morphology of the zinc borate and the differences in size and shape of the samples directly affected the filtration properties.

3.5. Experimental design results

The response surface methodology (RSM) was used to correlate the relationship among the effects of process variables that influence the particle size of zinc borate based on a three-level three-factor Box–Behnken design (BBD). Experimental data were analyzed using the Design Expert 10 statistical software [15]. The individual and combined effects of the process variables (temperature, stirring rate, and feed rate of the

reactants) on the average particle size of zinc borate were analyzed. The range and levels of the variables used in the experimental design are shown in Table 3.

The Box–Behnken matrix, experimental results of the combination of all the factors, and their corresponding responses for each run are given in Table 4.

Based on these results, the model equation as a function of the process variables obtained for the particle size of zinc borate crystals can be written as follows Eq. 1.

Where A is the temperature, B is the feed rate, and C is the stirring rate. The smallest particle size was obtained at 85°C, 300 mL/h, and 450 rpm. The fit and significance of the model and its coefficient were tested statistically by analysis of variance (ANOVA) [15], the results of which are given in Table 5.

The *p*-value was determined to evaluate the statistical significance of the model. The ANOVA results show a large F value of 64.17 and a small *p*-value < 0.05, which verify that the model fit is statistically significant. The precision of the model was checked by the use of the correlation coefficient (R^2), which was 0.9914, indicating a good correlation between the measured and predicted responses. The 'Pred R^2' value was in reasonable agreement with the "Adj R^2" value, with a difference of less than 0.12. Adeq Precision was used to measure the signal to noise ratio, with a value > 4 being desirable. In the present study, the signal to noise ratio was found to be > 4; therefore, the quadratic model could be used to navigate the design space. Moreover, a low coefficient of variation (CV) denoted good accuracy and reliability of the experiment. The independent process variables, temperature (A) and feed rate (B), and the second-order effect of temperature (A^2) and feed rate (B^2) on particle size were found to be significant ($p < 0.05$), whereas the other terms were insignificant ($p > 0.1$), as shown in Table 5.

The relationship between the particle size and the combined effect of two variables, namely temperature and feed rate, temperature and stirring rate, and feed rate and stirring rate at a constant level of the third variable are shown in Figure 7.

Each plot in Figure 7 shows the combined effect of two variables on the particle size with the third variable fixed. The tendency of each variable studied can be examined by evaluating the response of the surface. Figure 7 clearly shows that the average particle size of the zinc borate increased with increasing feed rate but decreased with increasing temperature. The contour plots are in accordance with the 3D-surface plots, revealing that the stirring rate had a negligible effect.

Table 3. Range and levels of the process variables.

Parameters	Factors	Levels		
		-1	0	1
Temperature (°C)	A	45	65	85
Feed Rate (ml/h)	B	300	600	900
Stirring Rate (rpm)	C	400	450	500

Table 4. Box–Behnken matrix and experimental results.

Run	Actual level of factors			Coded level of factors			Response
	Temperature (°C)	Feed Rate (mL/h)	Stirring Rate (rpm)	A	B	C	Particle size (μm)
1	65	300	400	0	-1	-1	4.8
2	65	900	400	0	+1	-1	6.5
3	65	300	500	0	-1	+1	4.6
4	65	900	500	0	+1	+1	6.2
5	45	300	450	-1	-1	0	5.5
6	45	900	450	-1	+1	0	7.9
7	85	300	450	+1	-1	0	3.3
8	85	900	450	+1	+1	0	5.2
9	45	600	400	-1	0	-1	6.3
10	45	600	500	-1	0	+1	6.0
11	85	600	400	+1	0	-1	4.0
12	85	600	500	+1	0	+1	3.5
13	65	600	450	0	0	0	5.4
14	65	600	450	0	0	0	5.4
15	65	600	450	0	0	0	5.4

$$Y_{PS} = 5.40 - 1.21A + 0.94B - 0.15C - 0.12AB - 0.050AC - 0.050BC - 0.26A^2 + 0.34B^2 - 0.19C^2 \quad (1)$$

Table 5. ANOVA results of the quadratic model for particle size.

Source	Sum of Squares	Df	Mean Square	F-Value	p-value Prob > F
Model	19.92	9	2.21	64.17	0.0001
A- Temperature (°C)	11.76	1	11.76	340.91	< 0.0001
B-Feed rate (ml/h)	7.03	1	7.03	203.80	< 0.0001
C- Stirring rate (rpm)	0.18	1	0.18	5.22	0.0712
AB	0.063	1	0.063	1.81	0.2361
AC	0.010	1	0.010	0.29	0.6134
BC	0.010	1	0.010	0.29	0.6134
A^2	0.25	1	0.25	7.37	0.0420
B^2	0.42	1	0.42	12.19	0.0174
C^2	0.13	1	0.13	3.76	0.1101
Residual	0.17	5	0.034		
Lack of Fit	0.17	3	0.057		
R^2	0.9914				

Adj R^2=0.9760, Pred R^2=0.8627, Adequate Precision = 28.353, CV% = 2.48, Standard Deviation = 0.19

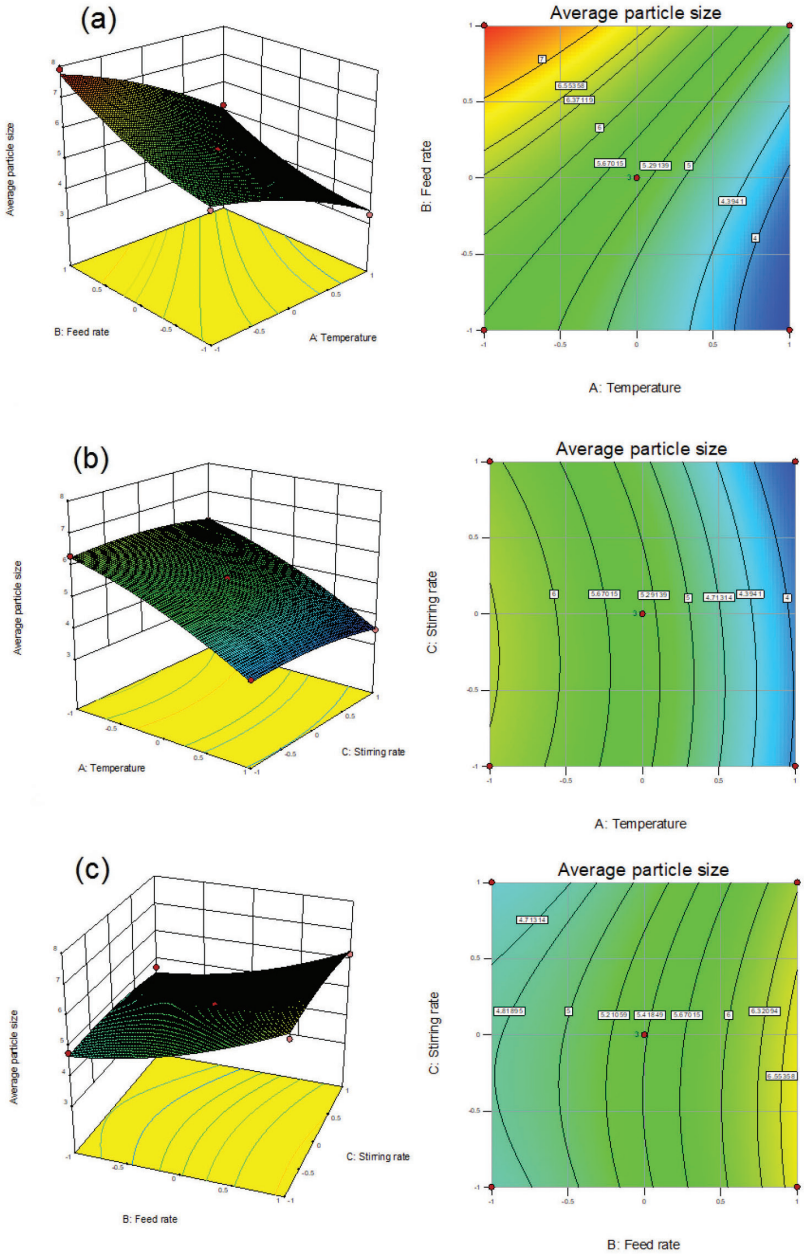

Figure 7. 3D-surface and contour plots showing the effect of a) temperature and feed rate; b) temperature and stirring rate; and c) feed rate and stirring rate on the average particle size of zinc borate crystals.

Both the surface and contour plots in Figure 7 show that a smaller particle size was obtained at a higher feed rate but a lower temperature. In comparison with the feed rate and stirring rate, temperature was the most significant variable affecting particle size.

4. Conclusions

This work assesses the effects of the operating conditions, including stirring rate, feed rate and temperature on zinc borate crystallization. The XRD, FTIR, and TGA/DTA results showed that all of the crystals were in the form of $Zn_2B_6O_{11}\cdot 7H_2O$. Microscopy analysis results indicated that operating conditions studied affected the size and crystal morphology. With decreasing feed rate and increasing temperature, the particle size of the zinc borate decreased distinctively. The changes in morphological characteristics in different operating conditions directly affected the filtration characteristics of zinc borate crystals. While the specific cake resistance of the zinc borate crystals obtained at 45 °C was calculated as 1.89×10^{10} m/kg, this value was determined as to 2.94×10^{10} m/kg for zinc borate at 85 °C. Moreover, Box–Behnken design with RSM was applied successfully to determine how temperature, feed rate, and stirring rate influenced the zinc borate crystallization in terms of the average particle size of the crystals. The model fit well to the experimental data, with an R^2 of 0.9914. Among the three investigated variables, temperature was the most efficient for creating a small crystal size. Consequently, the detailed information about the characterization and optimization could provide a reference for the crystallization of zinc borate for scientific and industrial purposes.

References

[1] Gostu S., Mishra D., Sahu K. K., Agrawal A., Precipitation and characterization of zinc borates from hydrometallurgical processing of zinc ash, Mater. Lett. 134 (1), 198-201, 2014.

[2] Bardakçı M., Acaralı N. B., Tuğrul N., Derun E. M., Pişkin M. B., Production of zinc borate for pilot scale equipment and effects of reaction conditions on yield, Mater. Sci. 19 (2), 159-163, 2013.

[3] Li S., Long B., Wang Z., Tian Y., Zheng Y., Zhang Q., Synthesis of hydrophobic zinc borate nanoflakes and its effect on flame retardant properties of polyethylene, J. Solid State Chem., 183, 957–962, 2010.

[4] Çakal G. Ö., Baltacı B., Bayram G., Özkar S., Eroğlu I., Synthesis of zinc borate using water soluble additives: Kinetics and product characterization, J. Cryst. Growth., 533, 125461, 2020.

[5] Liang P., Li S. Y., Synthesis, characterization and standard molar enthalpies of formation of two zinc borates: $2ZnO\cdot 2B_2O_3\cdot 3H_2O$ and ZnB_4O_7. J. Chem. Thermodyn., 139, 105868, 2019.

[6] Gürhan D., Çakal G. Ö., Eroğlu İ., Özkar S., Improved synthesis of fine zinc borate particles using seed crystals, J. Cryst. Growth., 311 (6), 1545-1552, 2009.

[7] Eltepe H.E., Balköse D., Ülkü S., Effect of temperature and time on zinc borate species formed from zinc oxide and boric acid in aqueous medium, Ind. Eng. Chem. Res., 46 (8), 2367- 2371, 2007.

[8] Shete A. V., Sawant S. B., Pangarkar V. G., Kinetics of fluid–solid reaction with an insoluble product: Zinc borate by the reaction of boric acid and zinc oxide, J. Chem. Technol. Biotechnol., 79 (5), 526-532, 2004.

[9] Gillani Q. F., Ahmad F., Mutalib M. I. A., Megat-Yusoff P. S. M., Ullah S., Messet P.J., Zia-ulMustafa M., Thermal degradation and pyrolysis analysis of zinc borate reinforced intumescent fire retardant coatings, Prog. Org. Coat., 123, 82-98, 2018.

[10] Savas L. A., Dogan M., Flame retardant effect of zinc borate in polyamide 6 containing aluminum hypophosphite, Polym. Degrad. Stabil., 165, 101-109, 2019.

[11] Tian Y., Guo Y., Jiang M., Sheng Y., Hari B., Zhang G., Jiang Y., et al., Synthesis of hydrophobic zinc borate nanodiscs for lubrication, Mater. Lett. 60 (20), 2511-2515, 2006.

[12] Zheng Y., Qu Y., Tian Y., Wang C. R. Z., Li S., Chen X., Ma Y., Effect of Eu^{3+}-doped on the luminescence properties of zinc borate nanoparticles, Colloid Surface A, 349 (1-3), 19-22, 2009.

[13] Gao Y. H., Liu Z. H., Synthesis and thermochemistry of two zinc borates, $Zn_2B_6O_{11}\cdot 7H_2O$ and $Zn_3B_{10}O_{18}\cdot 14H_2O$, Thermochim. Acta, 484, 27–31, 2009.

[14] Guo, Y. W., Mao L., Rong F., Li Z. H., Preparation of $Zn_3B_{10}O_{18}\cdot 14H_2O$ nanomaterials and their thermochemical properties, Thermochim. Acta, 539, 56– 61, 2012.

[15] Design-Expert software, Version 10 User's Guide, Stat-Ease.